IMPROVED RIDE-THROUGH OF PMSG WIND TURBINE DURING SYMMETRICAL VOLTAGE DIP USING A MAGNETIC AMPLIFIER

R. A. Ibrahim*, M.S. Hamad*, Khaled H. Ahmed[¶], Y. G. Dessouky*, and B.W. Williams[†]

* Arab Academy for Science and Technology, Egypt, rania_assem@alexseeds.com
[¶]Alexandria University, Egypt
[†] Strathclyde University, UK

Keywords: Low voltage ride through, permanent magnet synchronous generator, magnetic amplifier, voltage dip.

Abstract

Direct-drive wind turbines based on permanent magnet synchronous generator with full scale back to back converters are becoming very promising due to their high power density, gearless structure and flexible control. With the remarkable growth of wind energy capacity connected to the utility grids, strict grid interconnection requirements of power plants comprising permanent magnet synchronous generators technology are essential to improve the control of electrical power system, both in steady-state and transient operation. Low voltage ride through capability enhancement is one of the grid requirements which ensures the safe operation of the wind farm during the network disturbances and avoids its shutdown. This paper proposes an improved topology based on magnetic amplifier in the boost converter circuit to enhance the ride through capability of permanent magnet synchronous generators based wind energy systems.

Nomenclature

C_p	Performance coeff. for wind turbine
f	Supply frequency, (Hz)
i_b	Boost converter inductor current (A)
i_{dg}, i_{qg}	dq PMSG stator current components, (A)
i_a, i_b, i_c	Three phase grid currents, (A)
i_d, i_q	dq axis components of grid currents, (A)
i_d^*, i_q^*	dq reference grid current components, (A)
i_s	PMSG supply current, (A)
i_c	Magnetic amplifier control winding current, (A)
I_{inv}	Inverter IGBT current, (A)
I_{rec}	Rectifier diode current, (A)
L_f	Booster inductance, (H)
L_d, L_q	PMSG dq axis inductances, (H)
P_w	Power absorbed by windmill
P_{Grid}, Q_{Grid}	Grid active & reactive power, (Watt, VAR)
P_{Gen}, Q_{Gen}	PMSG active & reactive power, (Watt, VAR)
R_a	Stator armature resistance, (Ω)
R	windmill blade radius (m)
T_e	Electromagnetic torque, (N.m)

V	Wind velocity (m/sec)
V_{inv}	Inverter IGBT voltage, (V)
V_b	Input capacitor voltage of boost converter, (V)
V_{dc}	DC link capacitor voltage, (V)
V_{rec}	Rectifier diodes reverse voltage, (V)
v_a, v_b, v_c	Three phase grid voltages, (A)
ΔP_Q	Generator output increment (W)
ΔP_{grid}	Grid power increment (W)
ΔQ_C	Capacitor stored energy increment (J)
ΔV_{dc}	Incremental change in DC voltage
β	Blade pitch angle (BPA)
δ	Load angle, between q-axis and phase 'a' voltage, (rad)
φ_f	Permanent magnet flux linkage, (Wb)
φ_d, φ_q	dq axis flux-linkages, (Wb)
θ	Phase angle of grid voltage, (degree)
λ	Tip-speed ratio (TSR)
ρ	Air density
ω	Electrical rotor angular speed, (rad/s)

1 Introduction

Wind energy is considered as the largest producer of renewable energy. According to the Annual Energy Outlook, wind-powered generating capacity has grown over the past decade, from 18GW of installed capacity in 2000 to an estimated 179 GW in 2010 [1]. This large amount of variable generated power will bring issues such as power system operation; dynamic and steady state stability forcing the need for national regulatory grid codes. Within these regulations, low voltage ride through (LVRT) requirement for wind power plants have gained a great importance where the wind power system should stay connected to the grid for the grid fault conditions, contributing to keep network voltage and frequency stable by delivering active and reactive power to the grid [2]. In power systems where the wind power generation is of a major portion, the grid will experience huge power outage if the wind farms trip off [3], leading to instability in the power grid as well as destructive effects to the wind power converters.

Variable speed wind energy conversion systems (WECS) employing permanent magnet synchronous generators (PMSG) are one of the most popular wind energy configurations owing to their extended speed operating range,

high power density, full decoupling feature between the generator and the grid, and maximum energy capture at different wind speed. It is thus essential for grid operators to apply the LVRT regulations and rules to ensure successful ride through of PMSG when connected to the electrical utility grid. Methods for LVRT capability enhancement can be divided into ones requiring additional hardware to the WECS and others requiring change in the control system. Hardware solutions can be summarized as dynamic braking resistance (active crowbar), capacitor sizing, and energy storage systems [4, 5]. As for control techniques, LVRT capability enhancement can be achieved by modifications in the control strategy of the pitch controller, generator side, boost converter and grid side controllers [6]. These methods are explained thoroughly in [7] and has been extended to the farm level through the additions of FACTS compensation techniques [8]. In previous attempt by authors, LVRT capability enhancement was successful using a topology based on magnetic amplifiers found in [9]. The paper studied the impact of the addition of magnetic amplifier in DC link voltage limit as well as reducing the voltage and current stresses on the power converter switches.

In this paper, the authors further explore additional potentials of the topology by modifying the configuration thus reducing the overall size and cost of the proposed system. Simulation results can be found for the new proposed magnetic amplifier configuration. The new improved configuration shows promising results in limiting the DC link voltage rise, thus reducing the stresses on the power converters.

2 System Behaviour and Investigation

The WECS employed for grid connection of PMSG wind turbine can be found in figure 1 which consists of a drive train, PMSG, diode bridge rectifier, boost converter circuit and a voltage source inverter (VSI). A 16 kW, 690V PMSG grid connected system modelling have been carried out which includes aerodynamic model of the wind turbine using equations (1) to (4) and PMSG dynamic equations in *dq* frame using equations (5) to (7) [10] .

$$P_w = \frac{1}{2} \rho \pi R^2 V^3 C_p \qquad (1)$$

$$\lambda = \frac{\omega R}{V} \qquad (2)$$

$$C_p = 0.73 \left(\frac{151}{\lambda_1} - 0.58\beta - 0.2\beta^{2.14} - 13.2 \right) e^{\frac{-18.4}{\lambda_1}} \quad (3)$$

$$\lambda_1 = \frac{1}{\left(\frac{1}{\lambda - 0.02\beta} - \frac{0.08}{\beta^3 + 1} \right)} \qquad (4)$$

$$v_d = R_a i_d + L_d \frac{\partial i_d}{dt} - \omega L_q i_q \qquad (5)$$

$$v_q = R_a i_q + L_q \frac{\partial i_q}{dt} + \omega \varphi_f + \omega L_d i_d \qquad (6)$$

$$T_e = \frac{3}{2} \rho i_q \left(\left(L_q - L_d \right) i_d + \varphi_f \right) \qquad (7)$$

Boost converter circuit acts as the generator side converter and in this case is used for maximum power extraction from the wind and controls the rectifier output current [11]. Maximum power point extraction of wind for PMSG has been discussed in literatures [12-14]. Among these methods, optimal relationship based (ORB) technique has been used in this work as it lacks any wind speed measurement as well as its fast acting response to wind change. In this method, an optimal relationship is obtained between the boost inductor current i_b versus boost converter capacitor DC voltage v_b thus extracting maximum power at any given wind speed. Booster current is regulated using a PI controller followed by PWM modulator.

Grid side converter is based on three phase, two level 6 IGBT with anti parallel diode unit whose control is based on maintaining a fixed DC link voltage as well as exporting all the extracted power to the grid. Stationary *dq* axis currents are controlled where the active power is used in the inner loop to control the dc-link capacitor voltage. The reactive power is set to zero for unity power factor operation and is varied according to the grid requirements [15].

The system under investigation in figure 1 have been simulated and subjected to severe voltage dips (90% voltage dip for 140ms) as mentioned in the E-ON grid codes requirements [16] and simulation results are shown in figure 2 (a)- (g). During the voltage dip incidance at 2.5 sec, the grid power has fallen in response to the voltage dip while the PMSG extracted power will remain unchanged as seen from figures 2(f) and 2(g). Since the grid power has fallen to a very low value, the wind extracted power will be transformed into stored energy in the DC link capacitor causing rapid rise in its voltage (up to 1.2 pu) as well as high inrush currents (up to 7.5 pu) in the grid thus damaging the power converter units following the equation (8).

$$\Delta P_G - \Delta P_L = \Delta Q_C = \Delta V_{dc} \cdot I_{dc} = \Delta V_{dc} \cdot C \frac{dV_{dc}}{dt} \quad (8)$$

In larger MW wind turbines, similar voltage dips can cause much severe voltage rise as well as higher inrush currents depending on the capacitor size , dip voltage duration and network effective impedance.
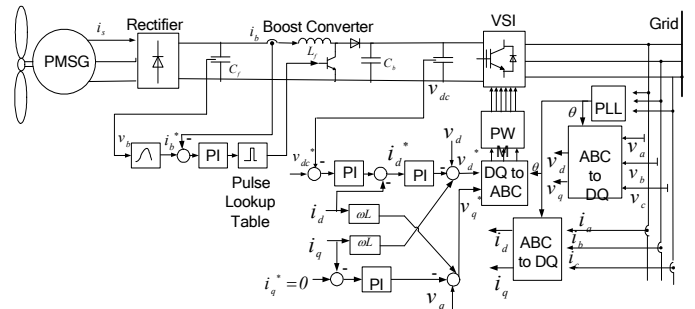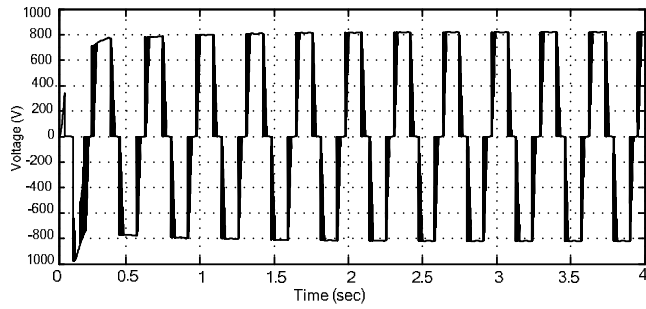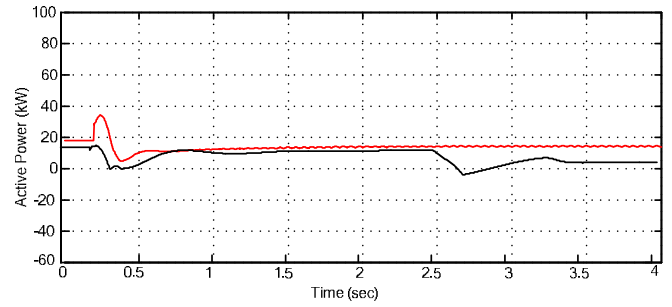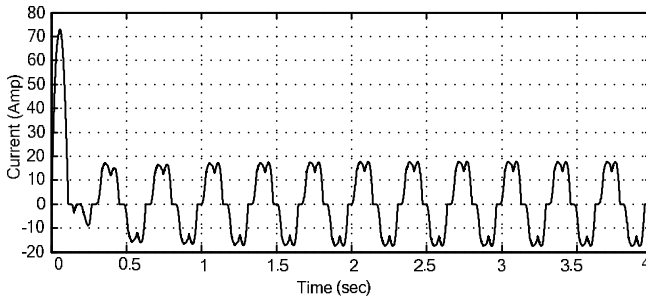

Figure 1: Block diagram for WECS using PMSG
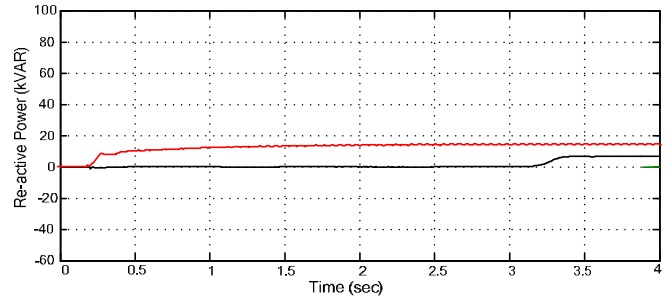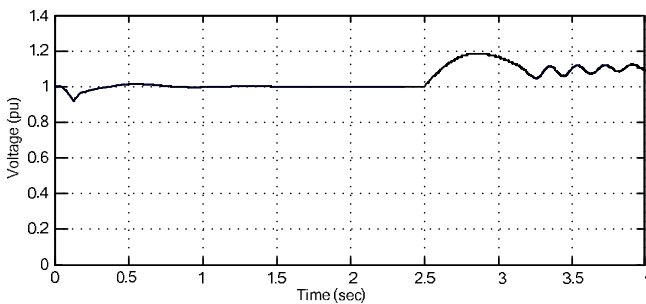
**(a)**

(b)

(c)

(d)

(e)

(f)

(g)

Figure 2: WECS behavior to 90% voltage dip without LVRT control. (a): Generator output voltage, (b): Generator output current, (c): DC link voltage, (d): DC link current, (e): Inverter current, (f): Generated and grid active power, (g): Generated and grid re-active power

3 Modified System Configuration using Magnetic Amplifier

Magnetic amplifiers have been used in applications such as instrumentation, relays, position servo mechanism, and automatic battery chargers owing to their high efficiency, reliability and ruggedness [17-19]. As explained in [9], magnetic amplifiers have the ability to control a large current signal (either AC or DC) flowing in its main winding through a small DC signal in the control winding by changing the magnetization characteristics of the magnetic core [20, 21]. In the first author's attempt, magnetic amplifiers were used in the configuration found in figure 2 as a method of series compensation when inserted between the PMSG and the diode rectifier (AC side configuration). In this configuration, each phase is split into two each having two magnetically coupled windings and a power diode. All six cores are being linked by a single biased DC controlled circuitry. During positive half cycle of the AC supply, the forward biased coils conduct thus transferring power to the load. Splitting each phase always produce an MMF in the DC circuit that are always cancelled out.

During normal grid operation (no voltage dips), if the DC control current i_c is such that it corresponds to the saturated part of the *BH* magnetization curve, then the mutual inductance between the AC and DC coil will be small causing a small voltage drop across the magnetic amplifier. On the other hand if a grid voltage dip occurred, the DC current i_c
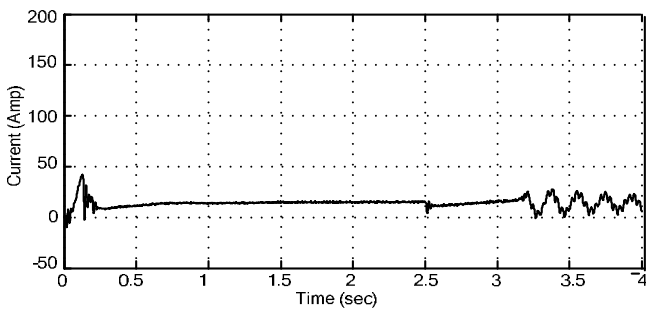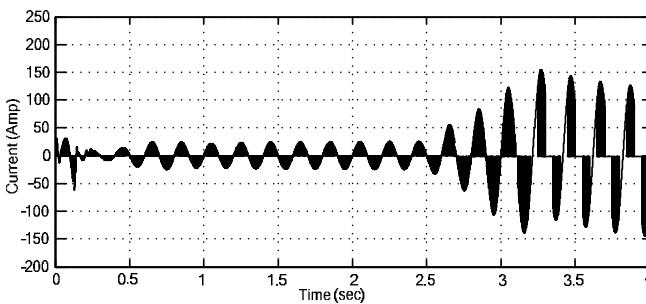
will cause the magnetic amplifier to operate in the linear part of the *BH* curve, then the magnetic amplifier will experience large voltage drop on its terminals limiting the DC link voltage rise. Results for the use of magnetic amplifier using the AC side configuration can be found in figure 4 (a) to (f) which proves that magnetic amplifier could be used in LVRT capability enhancement. The use of six magnetic elements and six power diodes added cost and size to the WECS which might be considered as one of the drawbacks of this approach.
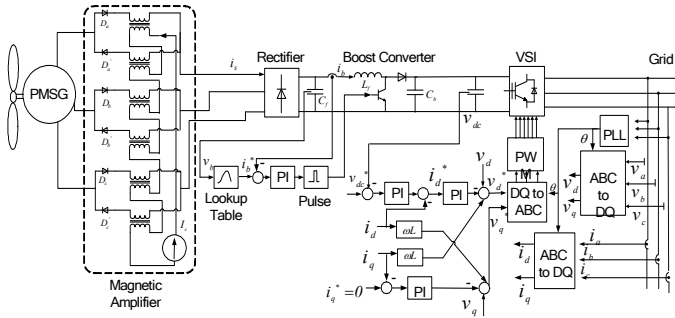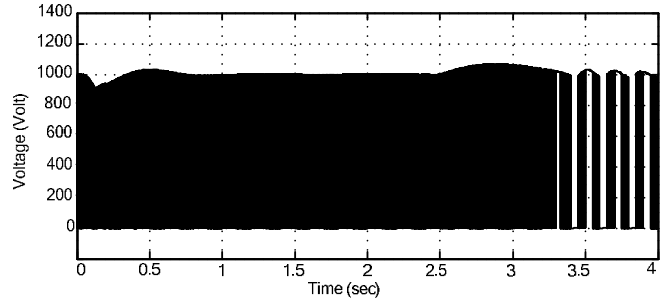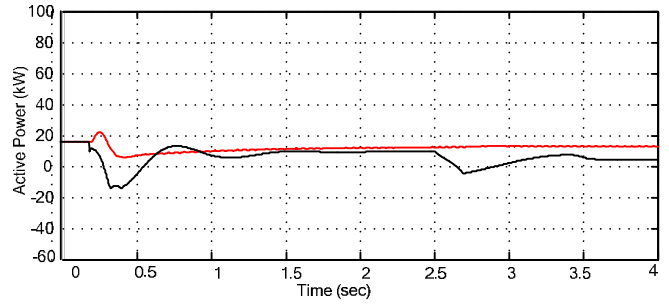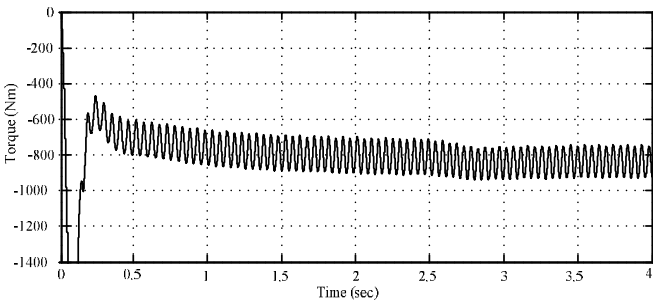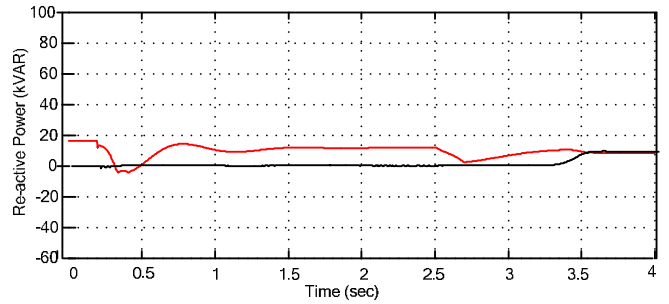
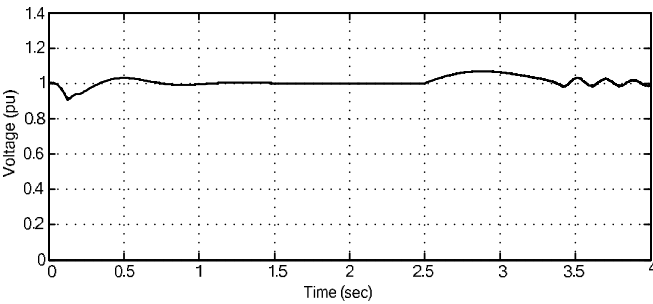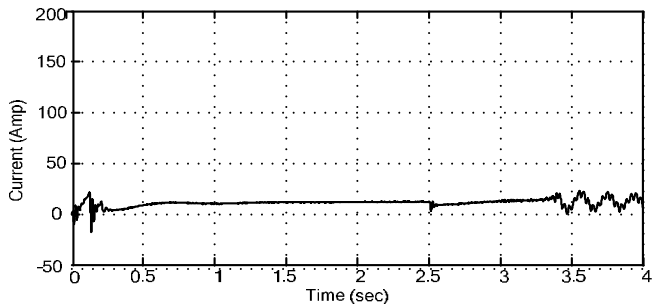Figure 3: WECS with magnetic amplifier in AC Side

(a)

(b)

(c)

(d)

(e)

(f)

Figure 4: WECS behavior to 90% voltage dip with magnetic amplifier in the AC side. (a): Electromagnetic torque, (b) DC link voltage, (c): DC link current, (d): Inverter voltage, (e): Generated and grid active power, (f): Generated and grid re-active power

Modifications have been made to the topology as to minimize the number of magnetic elements as much as possible yet still serving the same purpose for DC link voltage limit. The six magnetic amplifiers and six diodes where replaced by a single magnetic amplifier circuit added in the boost converter (DC side) as seen in figure 5. The principle of operation is the same as the AC side, when a fault occurs, the DC control current changes the operation of the magnetic amplifier from the saturated to the unsaturated state thus exhibiting larger voltage drop on its terminals. Simulation results for the DC side magnetic amplifier can be found in figure 6 (a) to (f).

Comparing the simulation results of magnetic amplifier in the AC side with the ones at the DC side proves the effectiveness of the DC side compensation. DC link voltage is being controlled and the stresses on the power converter semiconductor switches are being limited as seen in figure 5

and figure 6. The DC voltage oscillations present in the AC side configuration are being eliminated in the DC side one. Besides, magnetic amplifier addition in the DC link has eliminated the oscillations in the DC link current, which in turn will be reflected on the DC link power. As for the PMSG electromagnetic torque oscillations, it is observed that the PMSG exhibits stable operation with no effect on the electromagnetic torque at severe voltage dip.
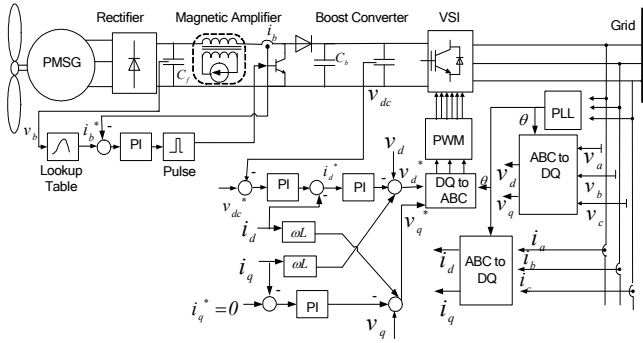

Figure 5: WECS with magnetic amplifier in DC Side
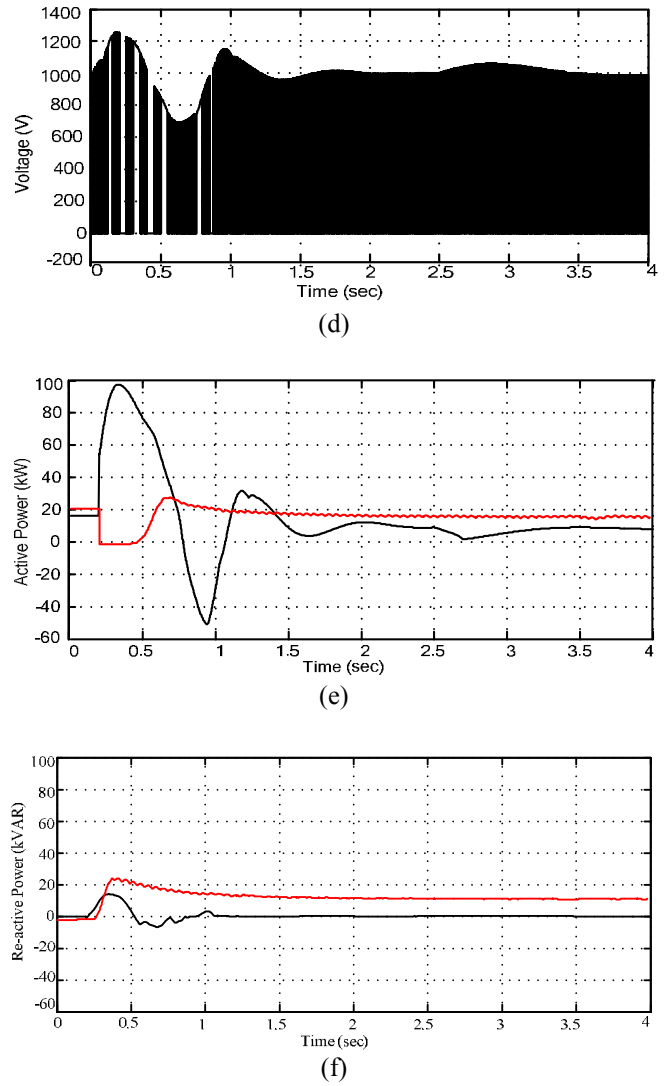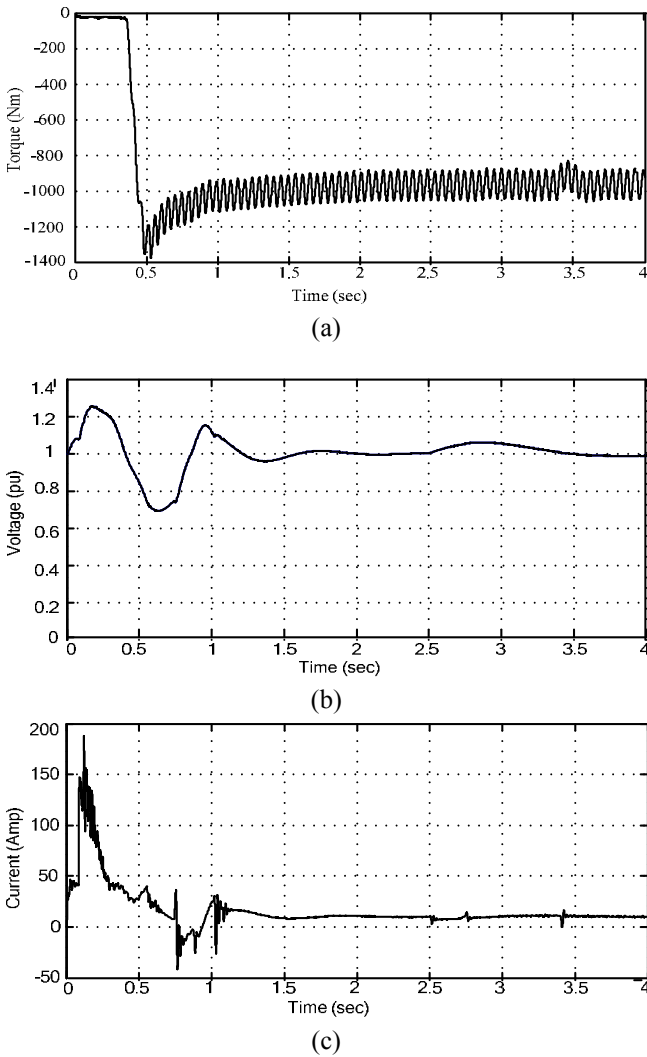

(a)

(b)

(c)

(d)

(e)

(f)

Figure 6: WECS behavior to 90% voltage dip with magnetic amplifier in the DC side. (a): Electromagnetic torque, (b) DC link voltage, (c): DC link current, (d): Inverter voltage, (e): Generated and grid active power, (f): Generated and grid re-active power

4 Conclusion

LVRT capability enhancement is considered one of the most important issues for grid connecting wind turbines to electrical grids. The problem is demonstrated with special focus on the effects on PMSG wind turbine systems, such as DC-link voltage rise as well as stresses on power electronic converters. Magnetic amplifiers have been suggested by authors in previous work to enhance the ride-through capability and this paper suggests modifications to the configuration reducing its size and overall cost. Simulation results are presented comparing both topologies and validating the idea.

References

[1] Annual energy outlook 2012 with projections to 2035 [Online]. Available: www.eia.gov/forecasts/aeo.

[2] G. Ramtharan, *et al.*, "Fault ride through of fully rated converter wind turbines with ac and dc transmission systems," *IET Renewable Power Generation,* vol. 3, p. 426, 2009.

[3] K. Ki-Hong, *et al.*, "Lvrt scheme of pmsg wind power systems based on feedback linearization," *IEEE Transactions on Power Electronics,,* vol. 27, pp. 2376-2384, 2012.

[4] A. Causebrook, *et al.*, "Fault ride-through of large wind farms using series dynamic braking resistors " *IEEE TRANSACTIONS ON POWER SYSTEMS* vol. 22, pp. 966-975, 2007.

[5] X. Hu, *et al.*, "Optimization of battery energy storage system with super-capacitor for renewable energy applications " *IEEE 8th International Conference on Power Electronics and ECCE Asia* (ICPE & ECCE), 2011, 2011.

[6] H. Shin, *et al.*, "Low voltage ride through(lvrt) control strategy of grid-connected variable speed wind turbine generator system," *IEEE 8th International Conference on Power Electronics and ECCE Asia* (ICPE & ECCE), 2011 2011.

[7] R. A. Ibrahim, *et al.*, "A review on recent low voltage ride-through solutions for pmsg wind turbine," in *International Symposium on Power Electronics, Electrical Drives, Automation and Motion (SPEEDAM), 2012* 2012, pp. 265-270.

[8] S. M. Muyeen, *et al.*, "Low voltage ride through capability enhancement of wind turbine generator system during network disturbance," *Renewable Power Generation, IET,* vol. 3, pp. 65-74, 2009.

[9] R. A. Ibrahim, *et al.*, "A novel topology for enhancing the low voltage ride through capability for grid connected wind turbine generators," in *IEEE Energy Conversion Congress and Exposition (ECCE), 2012*, 2012, pp. 2389-2395.

[10] R. Assem, *et al.*, "Parameters determination of grid connected interior permanent magnet synchronous generator," in *Power Electronics and Motion Control Conference (EPE/PEMC), 2012 15th International*, 2012, pp. DS1c.5-1-DS1c.5-6.

[11] R. Sharma, *et al.*, "Application of a synchronous generator with a boost converter in wind turbines: An experimental overview," *Renewable Power Generation, IET,* vol. 6, pp. 414-423, 2012.

[12] Y. Xia, *et al.*, "A new maximum power point tracking technique for permanent magnet synchronous generator based wind energy conversion system," *Power Electronics, IEEE Transactions on,* vol. 26, pp. 3609-3620, 2011.

[13] W. Quincy and C. Liuchen, "An intelligent maximum power extraction algorithm for inverter-based variable speed wind turbine systems," *IEEE Transaction on Power Electronics,* vol. 19, pp. 1242-1249, 2004.

[14] M. A. Abdullah, *et al.*, "A study of maximum power point tracking algorithms for wind energy system," in *IEEE First Conference on Clean Energy and Technology (CET)*, 2011, pp. 321-326.

[15] F. Blaabjerg, *et al.*, "Overview of control and grid synchronization for distributed power generation systems," *IEEE Transactions on Industrial Electronics,,* vol. 53, pp. 1398-1409, 2006.

[16] E. O. N. GmbH. High and extra high voltage, germany [Online]. Available: http://www.eon-netz.com

[17] C. Yie-Tone and D. Y. Chen, "Small-signal modeling of magnetic amplifier post regulators with current-mode control," *IEEE Transaction on Industrial Electronics,* vol. 47, pp. 821-831, 2000.

[18] K. Harada, *et al.*, "A novel high power factor converter using a magnetic amplifier," *IEEE Transactions on Magnetics* vol. 32, pp. 5013-5015, 1996.

[19] V. Yaskiv, "Using of high-frequency magnetic amplifier in switch mode dc power supplies," in *PESC 04. 2004 IEEE 35th Annual Power Electronics Specialists Conference*, 2004, pp. 1658-1662 Vol.2.

[20] C. W. Lufcy, "A survey of magnetic amplifiers," *Proceedings of the IRE* pp. 404-413, 1955.

[21] K. C. Parton, *et al.*, "Superconducting power-system transductor," *IEE Proceedings Generation, Transmission and Distribution,* vol. 128, pp. 235-242, 1981.